Journal of Alloys and Compounds 501 (2010) 204–210

Contents lists available at ScienceDirect

Journal of Alloys and Compounds

journal homepage: www.elsevier.com/locate/jallcom

High temperature synthesis of Sn–3.5Ag–0.5Zn alloy nanoparticles by chemical reduction method

C.Y. Lin[a,*], U.S. Mohanty[b], J.H. Chou[a]

[a] Department of Engineering Science, National Cheng Kung University, Tainan, 701, Taiwan
[b] Department of Applied Chemistry, National Chiao Tung University, Hsinchu, 300, Taiwan

ARTICLE INFO

Article history:
Received 11 February 2010
Received in revised form 29 March 2010
Accepted 2 April 2010
Available online 22 April 2010

Keywords:
Chemical reduction
Pb free solder nanoparticle
Sn–3.5Ag–0.5Zn alloy

ABSTRACT

The synthesis of Sn–3.5Ag–0.5Zn alloy nanoparticles was carried out respectively at 50 and 70 °C by using chemical reduction method to examine the temperature effect. The stirring times were 3, 12 and 24 h for each temperature. X-ray diffraction (XRD), scanning electron microscopy (SEM) and transmission electron microscopy (TEM) were used to investigate the microstructures of the nanoparticle alloys. X-ray diffraction patterns revealed that the compound of Ag_3Sn was formed in the alloying process. Other intermetallic compounds such as Ag_4Sn and Ag_5Zn_8 were also obtained in the XRD patterns. Results on TEM revealed that the isolated particles were spherical in shape and the particle size varied from 10 to 20 nm, showing the crystalline nature of the alloy. The nanoparticles obtained were evenly dispersed and less aggregated for the stirring time of 12 h and temperature of 50 °C. On the other hand, the nanoparticles obtained at 70 °C under the stirring time of 3 h were amorphous in nature and agglomerated which are reflected in the TEM micrographs.

1. Introduction

For a typical electronic product or system, its integrated circuit (IC) chips and electronic devices provide the necessary electronic interconnection as well as the mechanical support. Among them, solder joints provide the electrical and mechanical connections between silicon die I/O pads and the substrate bonding sites, and between the substrate and the PCB. The most widely used solders have been based on lead–tin alloys which are of low cost, high ductility, low surface tension and low eutectic temperature [1]. However, the toxicity of lead and its harmful effect on the environment has led to the development of Pb free solders. Some of the prominent Pb free solder alloys such as Sn–Zn, Sn–Sb, Sn–Bi, Sn–Ag and Sn–Ag–Bi have been reported [2–8].

Several methods have been used to produce solder alloys such as mechanical alloying and screen-printing techniques. However, these methods produce solders of relatively large size [9,10]. To meet the requirements for future electronic packaging technology, ultra small solder bumps of less than 100 μm pitch are a necessity [11,12]. The objective of the present research is to produce Sn–Ag–Zn alloy nanoparticles for lead-free bumping applications.

Several methods [13–17] have been used by scientists to synthesize nanoparticles. Chemical reduction is the most suitable and inexpensive method by which nanoparticles can be produced with controllable size and morphology. The choice of reducing agent [18,19] is the most important factor during chemical reduction process. The kinetics of formation and reaction temperature is also controlled by the reducing agent.

Monodispersive CoPt nanoparticles were synthesized by superhydride reduction of Co Cl_2 and $PtCl_2$ in diphenyl ether [20]. Sui et al. [21] have reported the synthesis of CoPt hard magnetic nanoparticle films by chemical reduction at higher temperature. The synthesis was carried out by hydrogen reduction of Co nitride and Pt chloride mixture. Ultra fine Fe Pt nanoparticles with particle size (2 nm) were produced by hexadecanediol reduction of iron acetyl acetonate in dioctyl ether [22]. Pb free Sn–3.5Ag–*X*Cu nanoparticles were synthesized by chemical reduction with $NaBH_4$. The isolated nanoparticles as observed by transmission electron microscopy (TEM) were spherical in shape and the particle size was about 10 nm [23]. Our research group also synthesized Sn–3.5Ag–*X*Zn alloy nanoparticles [24] by chemical reduction method using $NaBH_4$ as a reducing agent and poly-vinyl pyrrolidone (PVP) as a stabilizer. TEM results revealed that the isolated particles were spherical in shape and the particle size varied from 2 to 10 nm. However, there is not much literature available on the synthesis of Sn–3.5Ag–XZn alloy nanoparticles by chemical reduction technique at higher temperatures.

This paper focuses on the synthesis of Sn–3.5Ag–0.5Zn alloy nanoparticles at higher temperatures. It also investigates the morphology and crystal structure of the nanoparticles by using

* Corresponding author. Tel.: +886 62757575; fax: +886 6 2766549.
E-mail address: n9895121@mail.ncku.edu.tw (C.Y. Lin).

0925-8388/$ – see front matter © 2010 Elsevier B.V. All rights reserved.
doi:10.1016/j.jallcom.2010.04.111

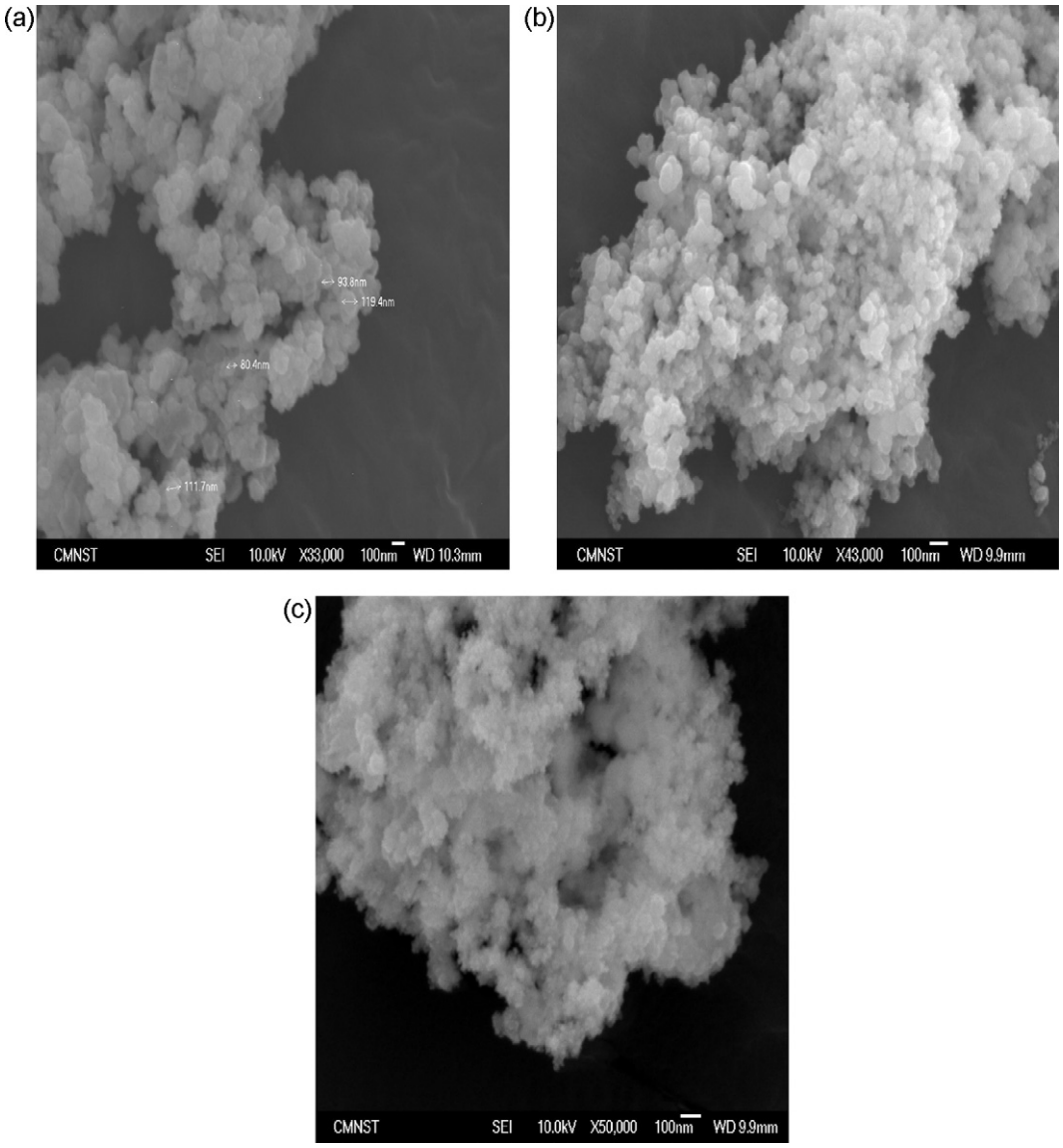

Fig. 1. SE micrograph of Sn–3.5Ag–0.5Zn nanoparticles synthesized at 50 °C for different stirring times (a) 3 h (b) 12 h (c) 24 h.

techniques such as TEM, scanning electron microscopy (SEM) and XRD. Many researches about lead-free solder alloys properties had been reported, Sn–Ag–Zn alloy has a melting point range of 218–221 °C which is lower than tin/lead eutectic [25–28].

2. Experimental approach

Sn–3.5Ag–0.5Zn alloy nanoparticles were synthesized by precipitation with 2.4 g $NaBH_4$ and 2 g PVP in 200 ml aqueous solutions at two temperatures, namely, 50 ± 3 and 70 ± 3 °C. The salts, $SnSO_4$, $AgNO_3$ and $Zn(NO_3)_2$ were procured from

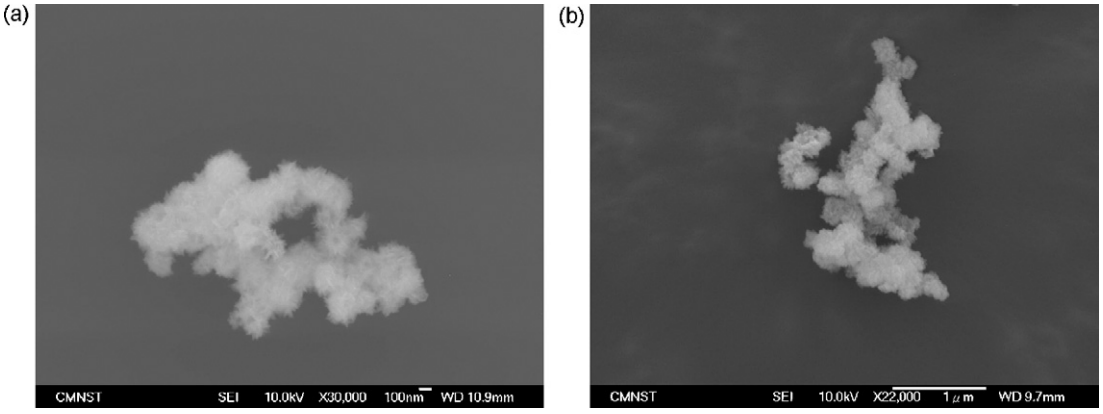

Fig. 2. SE micrograph of Sn–3.5Ag–0.5Zn nanoparticles synthesized at 70 °C for different stirring times (a) 12 h (b) 24 h.

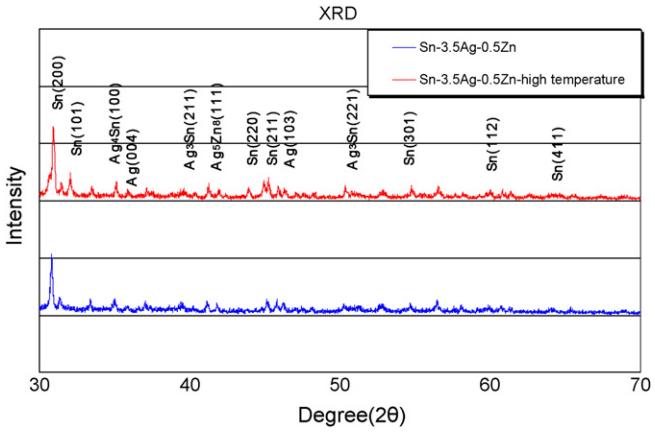

Fig. 3. X-ray diffraction patterns of Sn–3.5Ag–0.5Zn alloy nanoparticles synthesized at different temperatures.

Shimakyu's pure chemicals, Japan. These salts ($SnSO_4$: 3.47 g, $AgNO_3$: 0.11 g and $Zn(NO_3)_2$: 0.03 g) were dissolved in 50 ml aqueous solutions as metal precursors. The total weight of SnAgZn alloy was 2 g. Solutions of these precursors were added to sodium borohydride ($NaBH_4$) [Panreac Sintesis, 96%] and PVP (poly-vinyl pyrrolidone) [M.W., 40,000, Alfa Aesar] solution under constant stirring. The stirring of the solutions was performed at each temperature mentioned above. Two sets of solutions were prepared at temperatures of 50 and 70 °C, respectively. From each set, the solution containing the nanopowder was collected at stirring time of 3, 12 and 24 h. The collected samples, in the black precipitation form, were washed several times with distilled water until their pH value reached 7. Then the precipitate was filtered and dried in an oven maintained at a temperature of 40 °C for 12 h.

The nanoparticles/nanopowders obtained were characterized by an X-ray diffraction (XRD) for crystal structure and phase identification (XRD, Rigaku, DMAX-200/PC). The particle size, shape and morphology of the synthesized nanoparticles were observed with a field emission scanning electron microscope (JEOL, JSM-7000 F, Japan) and a transmission electron microscope (JEOL, JEM-2100, Japan). For the TEM (transmission electron microscopy) analysis, the particulate sample was dispersed in few milliliters of isopropanol in an ultrasonic bath and a drop of this dispersion was placed on a carbon film supported by a copper grid.

3. Results and discussion

3.1. Characterization of Sn–Ag–Zn nanoparticles by scanning electron microscopy

The SEM micrograph shown in Fig. 1 depicts the shape and morphology of Sn–3.5Ag–0.5Zn nanoparticles synthesized at tem-

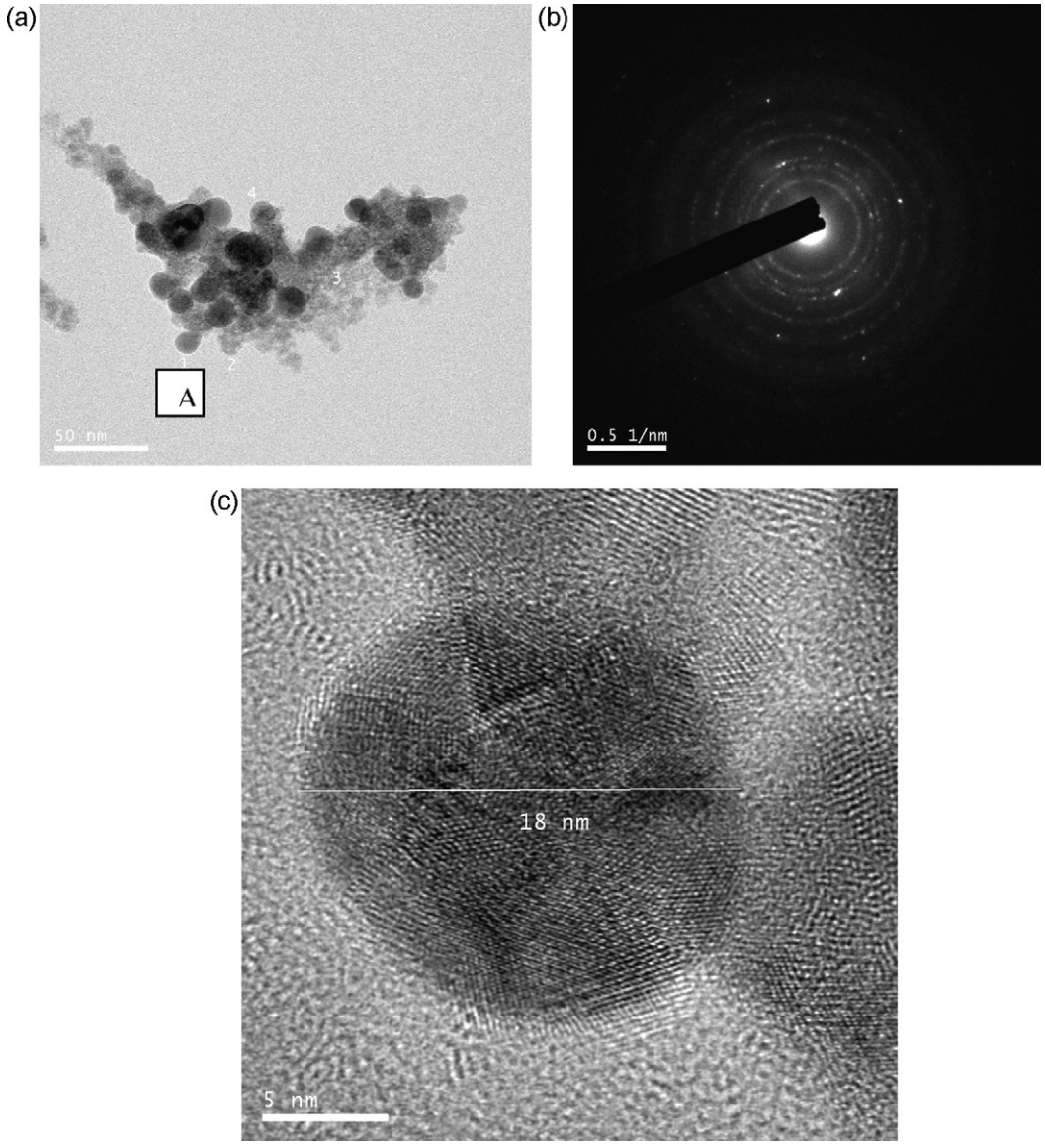

Fig. 4. Aggregation of Sn–3.5Ag–0.5Zn nanoparticle synthesized at 50 °C for a stirring time of 3 h (a) TEM image, (b) HRTEM image of magnified region A (c) SAED pattern.

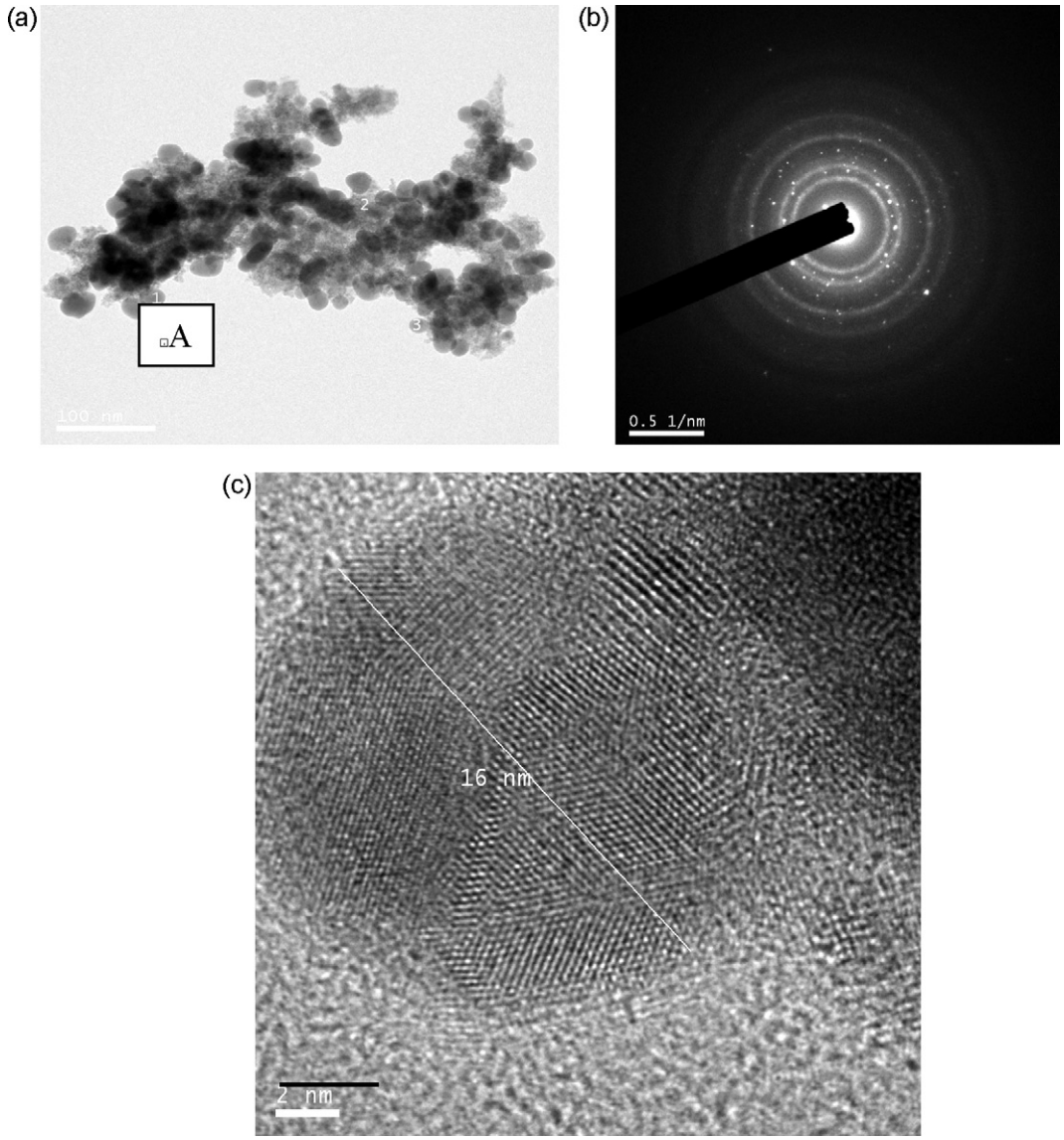

Fig. 5. Aggregation of Sn–3.5Ag–0.5Zn nanoparticle synthesized at 50 °C for a stirring time of 12 h (a) TEM image, (b) HRTEM image of magnified region A and (c) SAED pattern.

peratures 50 °C for different stirring times of 3, 12 and 24 h. It can be seen from Fig. 1a that for the stirring time of 3 h, a group of primary particles aggregated to form secondary particles. The average size of primary particles was in the range of 80–100 nm; however, it is difficult to obtain the accurate particle size due to the strong aggregation. On the other hand, the same particles synthesized at longer time (12 h) show different properties (Fig. 1b). They were more uniform, spherical in nature and dispersed more uniformly as compared to those shown in Fig. 1a. Apparently, the reaction time played an important role. At longer stirring time, greater number of nanoparticles was covered by PVP, so the aggregation of nanoparticles was reduced thus resulting in better dispersion. PVP has been used as a stabilizer [29] to synthesize various kinds of nanoparticles. Nemamcha and Rehspringer [30] obtained dispersed and aggregated palladium nanoparticles in the presence of ethylene glycol and poly-vinyl pyrrolidone. Further increase in the stirring time to 24 h resulted in greater dispersion of nanoparticles as depicted in Fig. 1c.

The mechanism of formation of nanoparticles has been proposed by Goia [31]. As per the mechanism the formation of metal atoms after mixing two solutions under strong stirring is caused by the transfer of electrons from a reducing agent (Red) to the oxidized metal species (Me^{n+}) as presented below:

$$Me^{n+} + Red^{m-} \leftrightarrow Me^{0} + Ox^{m-n} \quad (1)$$

Metal atoms produced as a result of electron transfer gradually associated themselves to form clusters. The clusters were basically dynamic entities involved in a continuous aggregation-dissociation process. They reached a critical size and formed nuclei when the critical supersaturation limit was exceeded and thus became stable entities of a metallic phase. The number and size of the nuclei generated in the solution was dependent on the redox potential of the reaction, temperature, concentration of reactants and properties of the solvent. Once the nuclei were formed they underwent a rapid diffusing growth at the expense of the remaining atoms in solution in excess of the saturation concentration and therefore formed larger nanosize primary particles. When more metal atoms were generated in the system, the primary particles continued to grow either by diffusion to form larger crystalline particles or depending on the experimental conditions they aggregated to form polycrystalline particles.

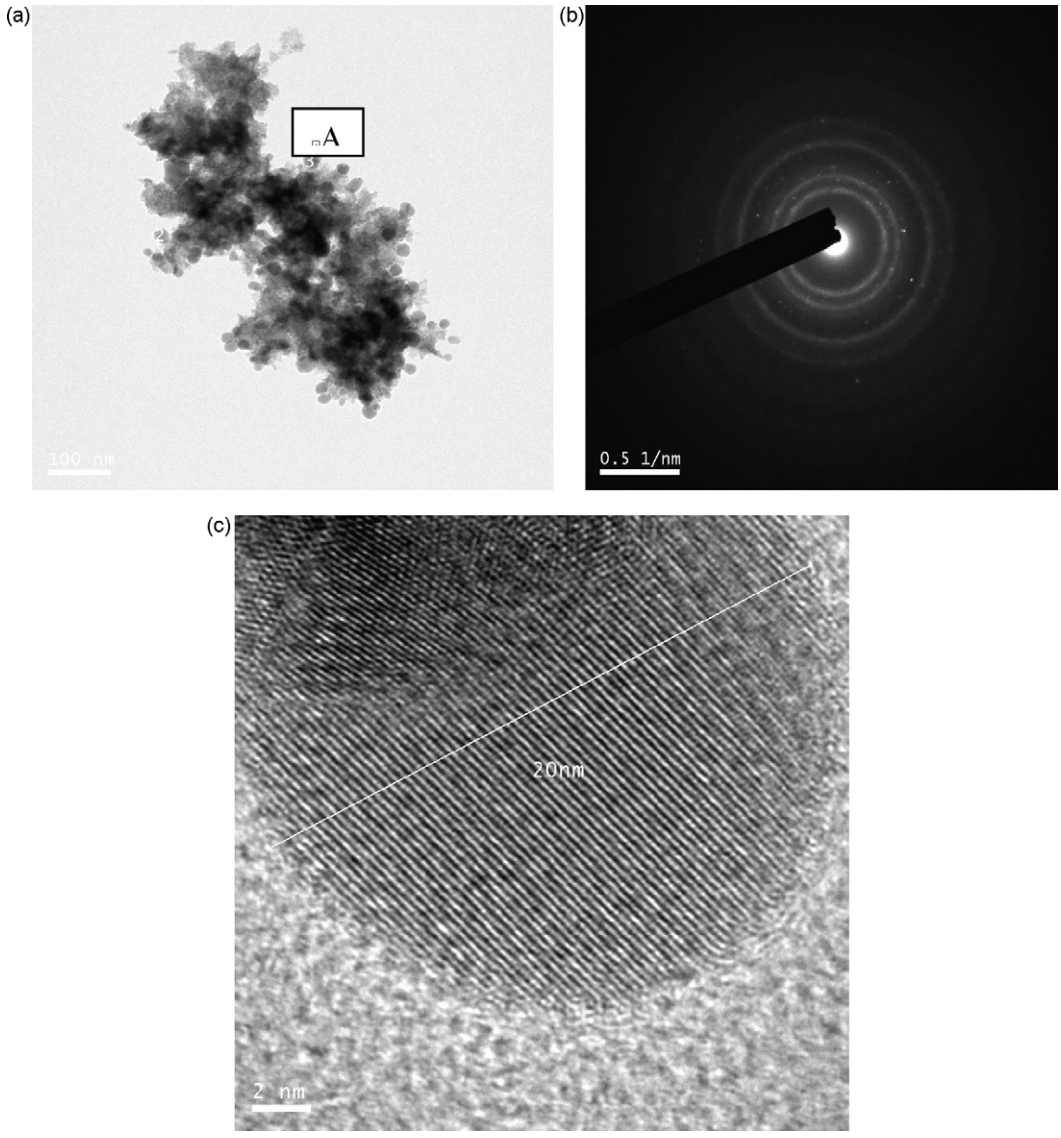

Fig. 6. Aggregation of Sn–3.5Ag–0.5Zn nanoparticle synthesized at 50 °C for a stirring time of 24 h (a) TEM image, (b) HRTEM image of magnified region A and (c) SAED pattern.

SE micrographs of Sn–3.5Ag–0.5Zn nanoparticles synthesized at 70 °C for different stirring times were shown in Fig. 2. Fig. 2a and b depicted the morphology of Sn–3.5Ag–0.5Zn nanoparticle synthesized at 70 °C for the stirring time of 12 and 24 h, respectively. The hairy like morphology can be observed from both figures and primary particles aggregated to form secondary particles resulting in large clusters. This indicated that synthesis of the Sn–3.5Ag–0.5Zn nanoparticles at this temperature lead to greater aggregation of particles.

3.2. Characterization of Sn3.5–Ag0.5–Zn alloy nanoparticles by X-ray diffraction (XRD) transmission electron microscopy (TEM) analysis

The crystal structure of Sn–3.5Ag–0.5Zn nanoparticle was investigated by XRD. Fig. 3 displays the XRD patterns of Sn–3.5Ag–0.5Zn nanoparticles synthesized at 25 °C (namely, room temperature) and 50 °C, respectively. For both temperatures, the XRD patterns for Sn–3.5Ag–0.5Zn alloy exhibited prominent peaks at scattering angles (2θ) of 30.9°, 32.2°, 44.01°, 45.25° and 55.2° which corresponded to scattering from (2 0 0), (1 0 1), (2 2 0), (2 1 1) and (3 0 1) crystal planes similar to the body center tetragonal phase of tin [32]. The other peaks for the tetragonal tin, i.e., Sn(1 1 2), Sn(3 2 1) and Sn(4 1 1) peaks were also observed at scattering angles (2θ) of 62.07°, 63.4° and 73.5°, respectively. In addition to the peaks indexed to the tetragonal cell of Sn with $a = 0.582$ and $c = 0.317$ nm, the Ag_3Sn phase at (39.7°) and (53.08°) were observed in the XRD patterns indicating the successful alloying of Sn and Ag by the reduction process [33]. There were also noticeable peaks of Ag_4Sn(1 0 0) and Ag_5Zn_8(1 1 1) obtained at 2θ value of 35.36° and 37.51°, respectively, in the XRD pattern. The formation of Ag_3Sn, Ag_4Sn and Ag_5Zn_8 in the diffraction pattern gave strong evidence that the nanoparticles were mixed homogenously. On the other hand, at 50 °C, the X-ray diffraction pattern showed an increase in the intensity of the major diffraction peaks. This indicated a change in morphology of Sn–3.5Ag–0.5Zn alloy nanoparticles at the higher temperature. Above 50 °C, there is no noticeable change in the XRD patterns.

Fig. 4 shows the TEM, SAED (selected area diffraction pattern) and HRTEM (high resolution transmission electron microscopy) images of the Sn–3.5Ag–0.5Zn alloy nanoparticles synthesized at 50 °C for the stirring time of 3 h. From the TEM image in Fig. 4a it can be noticed that the nanoparticles were spherical in shape and their size varied from 10 to 20 nm. The SAED diffraction pattern did not

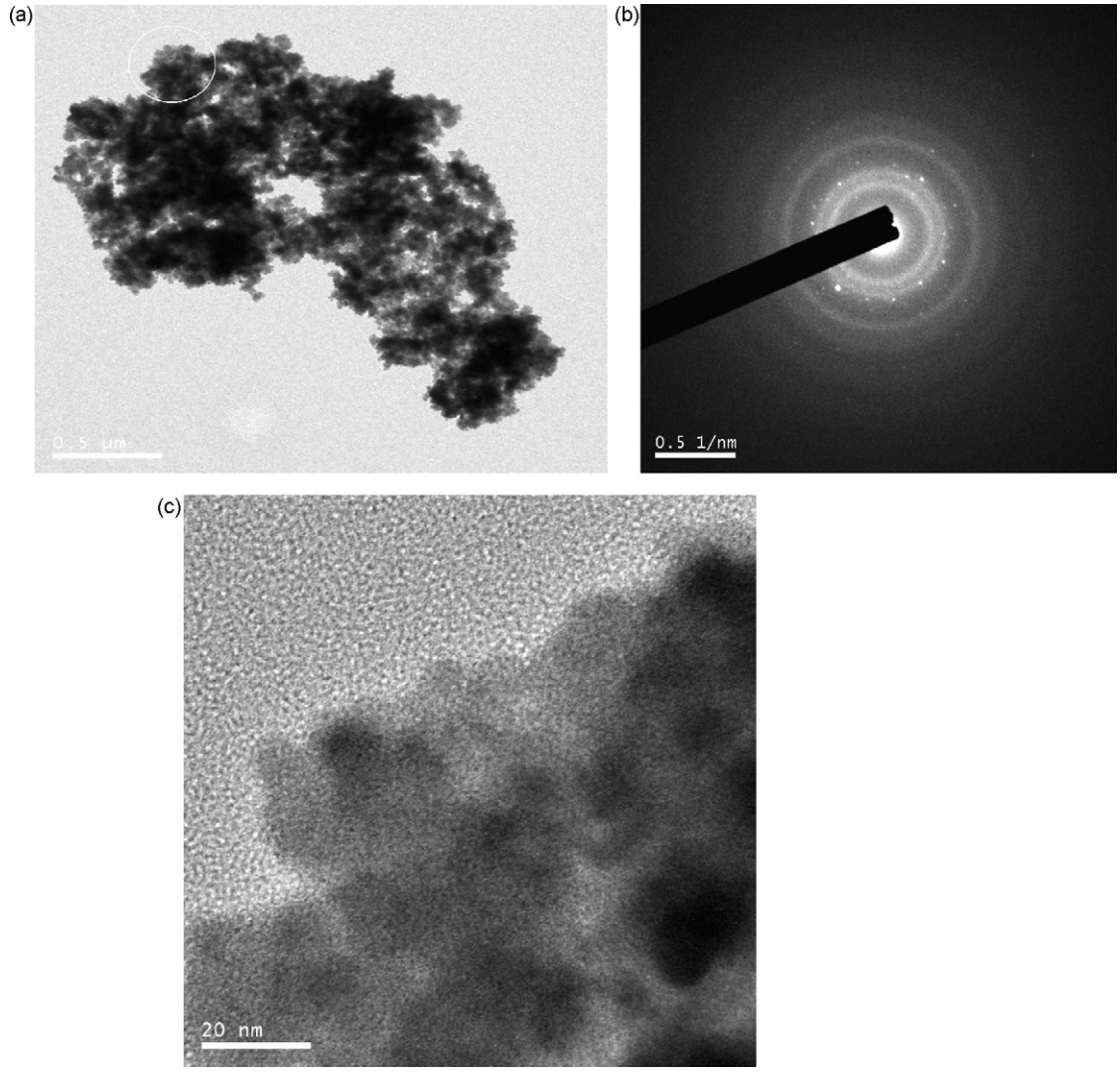

Fig. 7. Aggregation of Sn–3.5Ag–0.5Zn nanoparticle synthesized at 70 °C for a stirring time of 3 h (a) TEM image, (b) HRTEM image of magnified region A and (c) SAED pattern.

show uniform diffraction pattern which was attributed to the presence of a mixture of intermetallic compounds like Ag_3Sn, Ag_5Zn_8 and Sn of the tetragonal phase. The HRTEM image (Fig. 4c) of region A showed the particle size as 18 nm. However the lattice fringes were not uniform. They were aligned in different directions indicating the presence of an intermetallic compounds as mentioned above.

By contrast, from the TEM image shown in Fig. 5 it can be seen that the Sn–3.5Ag–0.5Zn nanoparticles obtained for the stirring time of 12 h were evenly dispersed and less aggregated as compared to those formed at the stirring time of 3 h. The results were consistent with those obtained by SEM illustrated in Fig. 1a and b. The SAED patterns (Fig. 5b) and HRTEM image (Fig. 5c) were brighter and the lattice fringes were more distinct compared to that shown in Fig. 4b suggesting that increasing in stirring time improved the crystallinity of Sn–3.5Ag–0.5Zn alloy nanoparticles. Increasing the stirring time to 24 h resulted in greater aggregation of particles as seen in TEM image in Fig. 6. The HRTEM image of the magnified region A showed the particle size as 20 nm and the SAED pattern indicated the presence of crystalline phases in the formed nanoparticle. There were also some dots seen in the SAED pattern indicating the presence of some polycrystalline nanoparticles. However, due to the strong aggregation of the growing particles, the phases could not be distinguished clearly.

Fig. 7 shows the TEM image of Sn–3.5Ag–0.5Zn alloy nanoparticles synthesized at 70 °C for the stirring time of 3 h. The result in Fig. 7a revealed that a large number of primary nanoparticles aggregated strongly to form secondary nanoparticles of larger sizes. HRTEM image (Fig. 7b) of the nanoparticles did not show the existence of any lattice fringes. The SAED diffraction pattern in Fig. 7c depicted a diffused circular ring suggesting that certain regions were amorphous.

Thus the final size of the metallic particle depends on the nucleation rate, the fraction of atoms involved in the formation of nuclei and the extent of the aggregation during the process. The synthesis of Pb free alloy nanoparticles at higher temperatures resulted in broader distribution of size of nanoparticles.

4. Conclusions

X-ray diffraction patterns revealed that Ag_3Sn was formed successful by the chemical reduction alloying process. Other intermetallic compounds such as Ag_4Sn and Ag_5Zn_8 were also obtained based on the XRD patterns. TEM results revealed that the isolated particles were spherical in shape and the particle size varied from 10 to 20 nm, indicating the crystalline nature of the alloy. The nanoparticles obtained were evenly dispersed and less aggregated for the stirring time of 12 h at the temperature of 50 °C. However,

the nanoparticles obtained at 70 °C under stirring of 3 h were amorphous in nature and the particles observed in the TEM and HRTEM were more aggregated.

References

[1] M. Abtew, G. Selvaduray, Mater. Sci. Eng. R. 27 (2000) 95.
[2] H.L. Lai, J.G. Duh, J. Electron. Mater. 32 (2003) 215.
[3] S.T. kao, J.G. Duh, J. Electron. Mater. 33 (2004) 1445.
[4] B.L. Young, J.G. Duh, B.S. Chion, J. Electron. Mater. 30 (2001) 543.
[5] S. Chada, R.A. Fournelle, W. Laub, D. Shanguan, J. Electron. Mater. 28 (1999) 1194.
[6] W. Yang, l.E. Felton, R.W. Messler Jr, J. Electron. Mater. 24 (1995) 1465.
[7] W.K. Choi, H.M. Lee, J. Electron. Mater. 28 (1999) 1251.
[8] U.R. Kattner, W.J. Boettinger, J. Electron. Mater. 23 (7) (1994) 603.
[9] I. Ohnuma, M. Miyashila, K. Azai, X.J. Liu, H. Ohtani, R. Kainuma, K. Ishida, J. Electron. Mater. 29 (2000) 1137.
[10] M. Kitajima, T. Shono, M. Takesue, M. Noguchi, K. Yamazaki, ICEP Proceedings, 2001, p. 72.
[11] R.R. Tummala, V.K. Madisetti, IEEE Des. Test. Comput. 16 (1999) 48.
[12] T. Ishii, S. Aoyama, J. Electron. Mater. 33 (2004) L21.
[13] M. Ojeda, S. Rojas, M. Botounet, F.J. Perez-Alonso, F.J. Garcia-Garcia, J.L.G. Fierro, Appl. Catal. A 274 (2004) 33.
[14] S. Karmakar, S. Taran, B.K. Chaudhuri, Phys. Status Solidi B 241 (2004) 3563.
[15] K.S. Chou, C.Y. Ren, Mater. Chem. Phys. 64 (2000) 41.
[16] K.D. Kim, D.N. Hou, H.T. Kim, Chem. Eng. J. 104 (2004) 55.
[17] Y. Zhu, Y. Qian, M. Zhang, Z. Chen, Mater. Letter. 17 (1993) 314.
[18] Z. Zhang, B. Zhao, L. Hu, J. Solid State Chem. 121 (1996) 105.
[19] K. Toroigoe, Y. Nakajima, K. Esumi, J. Phys. Chem. 97 (1993) 8304.
[20] S.C. Mu, H. Chao, Y.T. Zhong, X.C. Wen, E.S. Tang, D. Hao, G.H. Jun, Chin. Phys. Lett. 25 (2008) 1479.
[21] Y. Sui, L. Yue, R. Skomski, X.Z. Li, J. Zhou, D. sellmeyer, J. Appl. Phys. 93 (10) (2003) 7571.
[22] K.E. Elkins, G.S. Chaubey, V. Nandwana, J.P. Lin, J. Nanopart. Res. 3 (12) (2003) 1647.
[23] L.Y. Hsiao, J.G. Duh, J. Electrochem. Soc. 152 (9) (2005) J105.
[24] C.Y. Lin, U.S. Mohanty, J.H. Chou, J. Alloys Compd. 472 (2009) 281.
[25] N. Socolowski, Proceedings of Surface Mount International, 1995, p. 477.
[26] R. Keeler, EP&P (July) (1987) 45.
[27] K. Seelig, Circuit Assembly (October) (1995) 46.
[28] Cindy. Melton, SMT (June) (1995) 32.
[29] C.C. Yang, C.C. Wan, Y.Y. Wang, J. Electrochem. Soc. 153 (5) (2006) J27.
[30] A. Nemamcha, J.L. Rehspringer, Rev. Adv. Mater. Sci. 18 (2008) 685.
[31] D.V. Goia, J. Mater. Chem. 14 (2004) 451.
[32] Y. Zhao, Z. Zhang, H. Dang, Mater. Sci. Eng. A 359 (2003) 405.
[33] Y.B. Li, S. Zhang, T. Srithharan, Y. Liu, T.P. Chen, J. Alloys Compd. 457 (2008) 549.